Available online at www.sciencedirect.com

ScienceDirect

Ceramics International 40 (2014) 5019–5023

CERAMICS INTERNATIONAL

www.elsevier.com/locate/ceramint

Short communication

MnO_2-modified $0.98(K_{0.5}Na_{0.5})NbO_3$–$0.02LaFeO_3$ ceramics with low dielectric loss for high temperature ceramics capacitors applications

Hualei Cheng[a,*], Wancheng Zhou[a], Hongliang Du[a], Fa Luo[a], Dongmei Zhu[a], Boxi Xu[b]

[a]State Key Laboratory of Solidification Processing, Northwestern Polytechnical University, Xi'an, Shaanxi 710072, China
[b]School of Materials Science and Engineering, Nanyang Technological University, 50 Nanyang Avenue, 639798, Singapore

Received 3 July 2013; received in revised form 22 August 2013; accepted 23 August 2013
Available online 31 August 2013

Abstract

The MnO_2-doped $0.98(K_{0.5}Na_{0.5})NbO_3$–$0.02LaFeO_3$ [0.98KNN–0.02LF-x] lead-free ceramics were prepared by the conventional solid-state sintering method. The effects of MnO_2 doping on the phase structure, microstructure, and electrical properties of the ceramics were investigated. The results reveal that MnO_2 is an excellent sintering aid for the 0.98KNN–0.02LF-x ceramics to improve the densification and decrease the sintering temperature. Additionally, the MnO_2 doping significantly increases the dielectric permittivity and decreases the dielectric loss of the 0.98KNN–0.02LF ceramics. The 0.98KNN–0.02LF-1.5 mol% ceramics show excellent high temperature dielectric properties: the dielectric permittivity ε_r is approximately 2000 and dielectric loss $tg\delta$ is smaller than 3% at a broad temperature range from 100 to 400 °C.
© 2013 Elsevier Ltd and Techna Group S.r.l. All rights reserved.

Keywords: C. Dielectric properties; $(K_{0.5}Na_{0.5})NbO_3$; MnO_2; Microstructure

1. Introduction

High temperature multilayer ceramics capacitors (MLCC) are in great demand especially in the automotive electronics industry, which require that the high temperature dielectrics should provide a relative high, stable capacitance and low dielectric loss at a broad temperature range [1,2]. A number of high temperature dielectrics have been proposed in the past, among them $BaTiO_3$, $(Bi_{0.5}Na_{0.5})TiO_3$ and $(K_{0.5}Na_{0.5})NbO_3$ (KNN)-based ceramics demonstrating the increased interest in this field [3–11]. Especially, modified KNN ceramics such as, KNN–$(Ba_{0.5}Sr_{0.5})TiO_3$ [8], KNN–$Bi(Mg_{2/3}Nb_{1/3})O_3$ [10] and KNN–$Bi(Zn_{2/3}Nb_{1/3})O_3$ [11] show high relative permittivity at a broad temperature usage range. However, the dielectric loss still is higher than the $BaTiO_3$-based ceramics and need be reduced to meet the high temperature MLCC applications. Recently, our group and Zuo et al. confirmed that the $LaFeO_3$ doping facilitates the dielectric peak broaden and the $0.98(K_{0.5}Na_{0.5})NbO_3$–$0.02LaFeO_3$ ceramics show a broad dielectric peak with permittivity maximum near 1500 in the temperature range of 50–400 °C [12,13]. Unfortunately, the $0.98(K_{0.5}Na_{0.5})NbO_3$–$0.02LaFeO_3$ ceramics have a low bulk density of 4.03 g/cm^3 and high dielectric loss, which affect the electrical properties and are not beneficial to the high temperature MLCC application. It was noted that MnO_2 is an effective dopant in the Pb-containing piezoelectric ceramics to enhance the densification and reduce dielectric loss [14,15]. In addition, manganese has been used to improve the densification of the pure KNN ceramics [16]. Lin et al. also found that MnO_2 is an effective sintering aid for the KNN-based ceramics [17,18]. In order to further enhance the densification and reduce dielectric loss of $0.98(K_{0.5}Na_{0.5})NbO_3$–$0.02LaFeO_3$ ceramics, various quantities of MnO_2 were added into $0.98(K_{0.5}Na_{0.5})NbO_3$–$0.02LaFeO_3$ ceramics in the present study. The purpose of this paper is to investigate the effects of MnO_2 doping on microstructure and electrical properties of 0.98 $(K_{0.5}Na_{0.5})NbO_3$–$0.02LaFeO_3$ ceramics.

2. Experimental

$0.98(K_{0.5}Na_{0.5})NbO_3$–$0.02LaFeO_3+xMnO_2$ (abbreviated as 0.98KNN–0.02LF-x, $0 \le x \le 2.5$ mol%) ceramics were prepared by the conventional solid-state reaction method. The stoichiometric $0.98(K_{0.5}Na_{0.5})NbO_3$–$0.02LaFeO_3$ powders were first synthesized at 950 °C for 5 h by a solid-state reaction. After the calcinations, $0.98(K_{0.5}Na_{0.5})NbO_3$–$0.02LaFeO_3$ and MnO_2 powders were weighed according to the formula of 0.98KNN–0.02LF-x ($0 \le x$

*Corresponding author. Tel.: +86 029 88494574; fax: +86 029 88494574.
E-mail address: hualeicheng@163.com (H. Cheng).

0272-8842/$ - see front matter © 2013 Elsevier Ltd and Techna Group S.r.l. All rights reserved.
http://dx.doi.org/10.1016/j.ceramint.2013.08.095

≤2.5 mol%) and then ball milled for 12 h. The dried mixtures were pressed into disks of 12 mm in diameter and 1 mm in thickness and then were sintered at 1130–1150 °C for 2 h. The obtained samples were polished. Silver paste was fired on both sides of the samples at 810 °C for 20 min as the electrodes for the sake of measurements.

The phase structures of the sintered ceramics were examined using X-ray powder diffraction analysis with a Cu Kα radiation (Philips X-Pert ProDiffractometer, Almelo, and The Netherlands) at room temperatures. The microstructure evolution was observed using a scanning electron microscopy (SEM) (model JSM-6360, JEOL, Tokyo, Japan). The dielectric spectrum measurements were performed using the LCR meter (Agilent E4980, USA) with a heat rate of 3 °C/min in a temperature range of 25–520 °C. The polarization versus electric (*P–E*) hysteresis loops was observed using a radiant precision workstation.

3. Results and discussion

Fig. 1 shows the variations of the bulk density (ρ) and optimum sintering temperature (T_s) of 0.98KNN–0.02LF-x ceramics as a function of the MnO_2 content x. The optimum sintering temperature is determined as the sintering temperature at which the ceramic has the largest density [8]. As shown in Fig. 1, the 0.98KNN–0.02LF-x ceramics with $x=0$ (e.g., without MnO_2 doping) have a low bulk density of 4.03 g/cm^3. After a small amount of MnO_2 ($\geq$0.5 mol%) is added, the bulk density of the ceramics increases at first and reaches a maximum value of 4.31 g/cm^3 when the MnO_2 content x is 1.5 mol%, then decreases gradually. In addition, as the MnO_2 content x increases, the optimum sintering temperature for the 0.98KNN–0.02LF-x ceramics decreases continually. The optimum sintering temperature for the 0.98KNN–0.02LF-x ceramics with $x=0$ and $x=2.5$ mol% are 1150 °C and 1130 °C, respectively. Obviously, MnO_2 acts as an excellent sintering aid to improve the densification and decrease the sintering temperature for the 0.98KNN–0.02LF-x ceramics.

Fig. 2 shows the SEM micrographs of the 0.98KNN–0.02LF-x ceramics sintered at the optimum temperature. As shown in Fig. 2(a), although the sintering temperature is high (1150 °C), the 0.98KNN–0.02LF-x ceramics with $x=0$ have a loose microstructure and a large amount of pores can be found in the grain boundary. The grains size of the 0.98KNN–0.02LF-x ceramics is about 1.0 μm when the MnO_2 doping is absent. However, the ceramics can be well sintered after a small amount of MnO_2 ($\geq$0.5 mol%) is added, which become considerably dense and the grains size becomes distinctly smaller and more uniform (Fig. 2b–c). Particularly, as the MnO_2 content x is equal to 2.5 mol%, the formation of a liquid phase is observed at the grain boundary as shown in Fig. 2(c). The formation of a liquid phase is critical for densification of KNN-based ceramics and which is responsible for the increased relative density [19]. However, the bulk density of the 0.98KNN–0.02LF-2.5 mol% ceramics slightly decreases in our studies. The possible reasons for the decreased density are as follows: at higher MnO_2 doping level (1.5 mol%), MnO_2 continues decreasing the sintering temperature of the ceramics with the formation of a liquid phase. On the other hand, the excess liquid phase can also weak the densification effect and decrease the density, the similar phenomena have also been observed in other KNN systems [19,20]. As a result, the density reaches a maximum and then slightly decreases rather than increases continuously with further increasing the MnO_2 content.

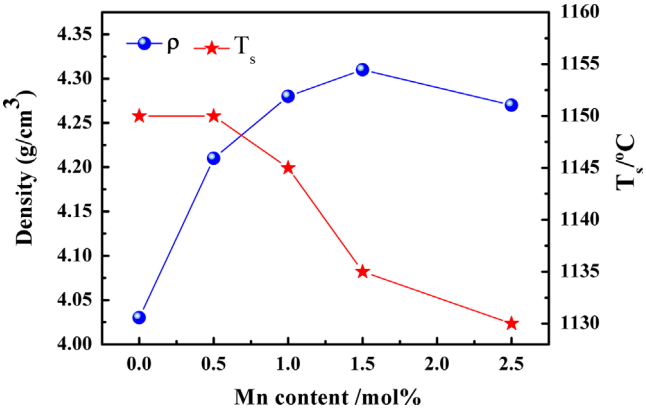

Fig. 1. Variations of the bulk density (ρ) and optimum sintering temperature (T_s) of 0.98KNN–0.02LF-x ceramics as a function of the MnO_2 content x.

Fig.3 shows the XRD patterns of 0.98KNN–0.02LF-x ceramics sintered at the optimum temperature. It can be seen that all the ceramics possess a pure perovskite structure without any detectable secondary phases, suggesting that LF has completely diffused into the KNN lattice to form a new solid solution, and the corresponding XRD patterns can be indexed in Refs. [12] and [13]. With increasing the MnO_2 content x, the phase structures of 0.98KNN–0.02LF-x ceramics do not show any significant change and the similar phenomenon also can be observed in other KNN ceramics modified with MnO_2 [17,18].

The temperature dependence of the dielectric permittivity and dielectric loss at 10 kHz for 0.98KNN–0.02LF-x ceramics are shown in Fig. 4. Similar to the pure KNN ceramics [8], the 0.98KNN–0.02LF-x ceramics undergo two phase transitions: the paraelectric cubic-ferroelectric tetragonal phase transition (T_C) and the ferroelectric tetragonal-ferroelectric orthorhombic phase transition (T_{O-T}). Differently, both of these phase transitions become broaden and the 0.97KNN–0.02LF ceramics exhibit a very stable temperature dependence of dielectric permittivity with permittivity maximum near 2000 in the temperature range of 100–400 °C. After a small amount of MnO_2 ($\geq$0.5 mol%) is added, the dielectric permittivities (ε_m) of the ceramics are higher than the 0.98KNN–0.02LF ceramics and the values of the dielectric peak at T_C increase significantly, indicating that the ferroelectric–paraelectric phase transition at T_C become stronger. It is found from Fig. 4(b) that the dielectric loss of all samples are lower than 5% even at the temperature as high as 300 °C. The room temperature dielectric loss (tan $\delta_{(RT)}$) of the 0.98KNN–0.02LF-x ceramics become much lower (less than 3%) after the doping of a small amount of MnO_2 as presented in the inset of Fig. 4(b). Moreover, with increasing the MnO_2 content x, the tan $\delta_{(RT)}$ reaches a minimum value at $x=1.5$ (~2.3%). The great decrease in tan $\delta_{(RT)}$ should be ascribed to the neutralization of

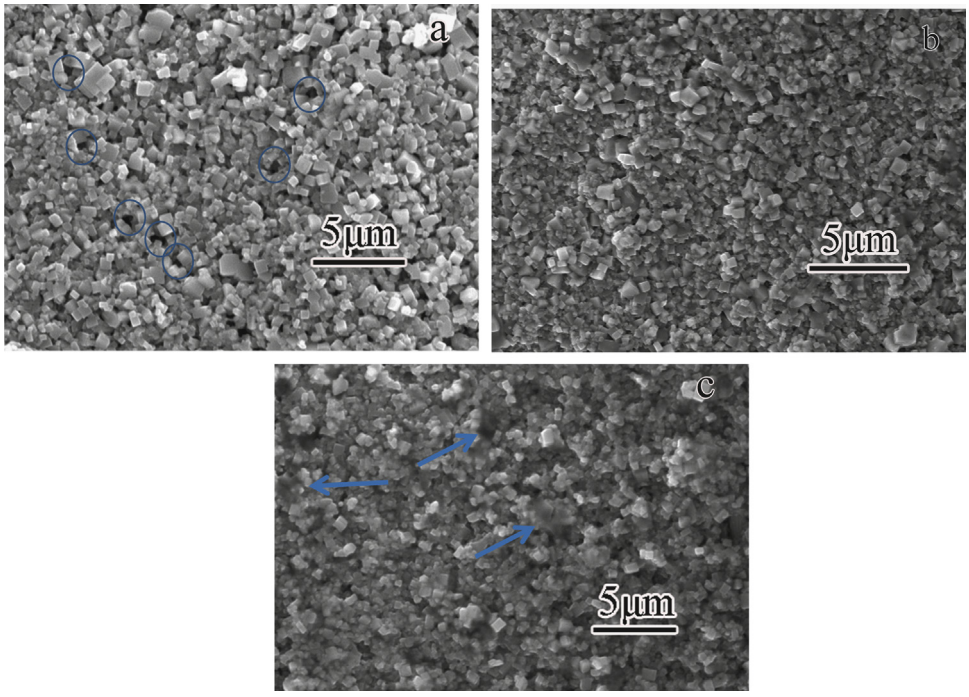

Fig. 2. (a–c) SEM micrographs of the 0.98KNN–0.02LF-x ceramics sintered at the optimum temperature: (a) $x=0$ (i.e., without MnO_2-doping), sintered at 1150 °C for 2 h, (b) $x=1.5$ mol%, sintered at 1135 °C for 2 h, and (c) $x=2.5$ mol%, sintered at 1130 °C for 2 h.

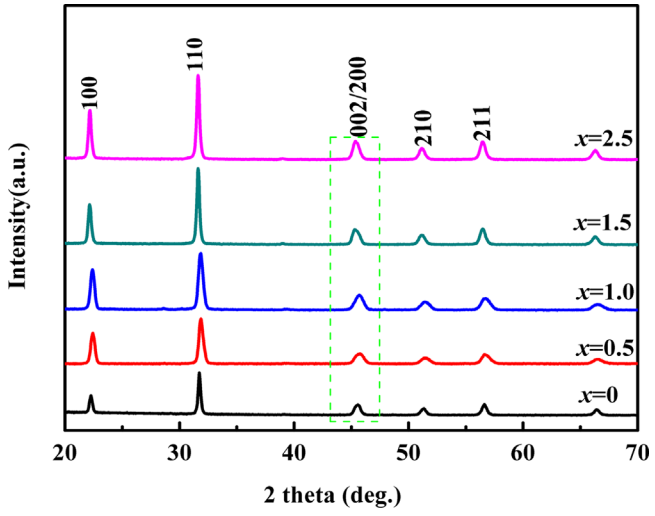

Fig. 3. XRD patterns of 0.98KNN–0.02LF-x ceramics sintered at the optimum temperature.

oxygen vacancies' action by the introduction of MnO_2 and the enhancement in densification. Before diffusing into lattice, MnO_2 will decompose to a state with Mn^{2+} or Mn^{3+} (0.83 Å or 0.65 Å) at a very low sintering temperature [21]. According to the principles of crystal chemistry and radius-matching rule, it is reasonable that the B-site of Nb^{5+} and Fe^{3+} (0.64 Å and 0.65 Å) are occupied by Mn ions, therefore, it is possible to result in the acceptor characteristic and create oxygen vacancies to maintain the electrical neutrality due to aliovalent substitutions. The defect dipoles are created when oxygen vacancies combine with Mn ions. These defect dipoles move along the direction of polarization, and the "hard" doping effects are created based on the principle of symmetry conforming of point defects, therefore, the doping of a small amount of MnO_2 decreases effectively tan $\delta_{(RT)}$.

The data of T_C, T_{O-T}, relative room temperature dielectric permittivity $\varepsilon_{r(RT)}$, tan $\delta_{(RT)}$, the remanent polarization $2P_r$ and the coercive field $2E_C$ of the 0.98KNN–0.02LF-x ceramics sintered at the optimum temperature measured at 1 kHz are listed in Table 1. From the table, it can be seen that the $2P_r$ continually decreases, whereas $2E_C$ increases slightly with increasing x from 0.5 to 1.5 mol%. The decrease in $2P_r$ suggests that the addition of MnO_2 would weaken the ferroelectricity of the ceramics. Similar weakening effects have also been reported for MnO_2 modified KNN-based ceramics, such as $MnCO_3$-modified $(Li_{0.04}K_{0.52}Na_{0.44})(Nb_{0.86}Ta_{0.1}Sb_{0.04})O_3$ ceramics [22] and MnO_2-doped $0.94(K_{0.5}Na_{0.5})NbO_3$–$0.06Ba(Zr_{0.05}Ti_{0.95})O_3$ ceramics [18]. The increase in $2E_C$ may be attributed to the pinning effect of domain walls due to the increase in the number of oxygen vacancies generated the acceptor-type doping of MnO_2 [18]. On the other hand, the increased density that diminishes the leakage current enhancing the polarization in process may be another reason for the enhanced $2E_C$ [23].

4. Conclusion

Normally sintered 0.98KNN–0.02LF-x ceramics with high density were obtained. The MnO_2 doping increases the dielectric permittivity and decreases the dielectric loss of the 0.98KNN–0.02LF ceramics. The decreased dielectric loss should be ascribed to the "hard" doping effects by the introduction of MnO_2 and the enhancement in densification. The $0.98(K_{0.5}Na_{0.5})NbO_3$–0.02 $LaFeO_3$-1.5 mol% ceramics show excellent dielectric properties: ε_{max} is near 2000, $tg\delta$ is lower than 3% at a broad temperature

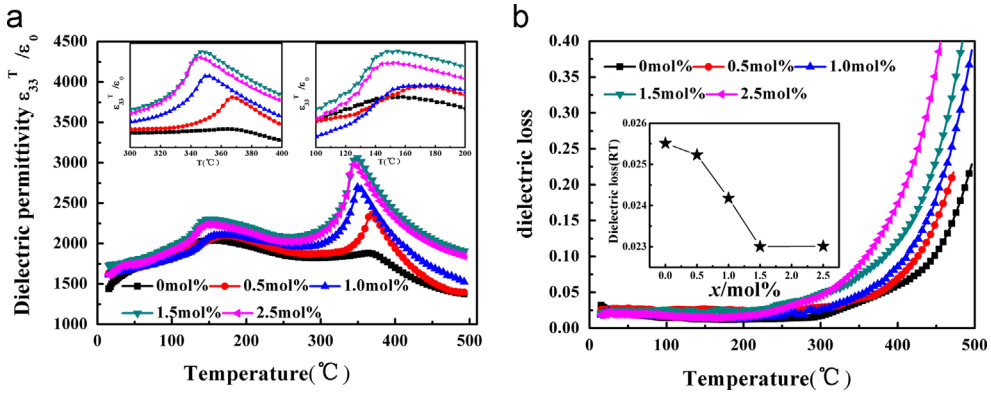

Fig. 4. Temperature dependence of dielectric permittivity and dielectric loss for 0.98KNN–0.02LF-x ceramics sintered at the optimum temperature.

Table 1
Summary of parameters of 0.98KNN–0.02LF-x ceramics sintered at the optimum temperature.

Samples	T_C(°C)	T_{O-T}(°C)	$\varepsilon_{r(RT)}$	tan $\delta_{(RT)}$	$2P_r$ (μC/cm^2)	$2E_c$ (kV/mm)
0	375	167	1547.3	0.026	–	–
0.5	366	165	1671.6	0.025	45.9	3.74
1	351	155	1644.5	0.024	36.7	4.04
1.5	347	147	1749.2	0.023	21.9	4.52
2.5	345	145	1685.2	0.023	12.1	2.7

usage range from 100 to 400 °C, which indicate the potential application in high temperature MLCC field.

Acknowledgments

This work was supported by the Doctorate Foundation of Northwestern Polytechnical University (No CX201108), the National Natural Science Foundation of China (Grant no. 51072165), and the fund of State Key Laboratory of Solidification Processing in NWPU (No. KP 201307).

References

[1] R.W. Johnson, The changing automotive environment: high-temperature electronics, IEEE Transactions on Components, Pack Aging, and Manufacturing Technology 27 (2004) 164–176.
[2] R. Dittmer, J. Wook, D. Damjanovic, Lead-free high-temperature dielectrics with wide operational range, Journal of Applied Physics 109 (2011) 034107.
[3] R. Dittmer, E.M. Anton, Jo Wook, A high-temperature-capacitor dielectric based on $K_{0.5}Na_{0.5}NbO_3$-modified $Bi_{1/2}Na_{1/2}TiO_3$–$Bi_{1/2}K_{1/2}TiO_3$, Journal of the American Ceramic Society 95 (2012) 3519–3524.
[4] N. Raengthon, T. Sebastian, D. Cumming, $BaTiO_3$–$Bi(Zn_{1/2}Ti_{1/2})O_3$–$BiScO_3$ ceramics for high-temperature capacitor applications, Journal of the American Ceramic Society 95 (2012) 3554–3561.
[5] C.C. Kruea-In, G. Rujijanagul, F.Y. Zhu, Relaxor behaviour of $K_{0.5}Bi_{0.5}TiO_3$–$BiScO_3$ ceramics, Applied Physics Letters 100 (2012) 202904.
[6] Z.P. Yang, X.L. Chao, Z. Li, Phase structures, electrical properties and temperature stability of $(1-x)[(K_{0.458}Na_{0.542})_{0.96}Li_{0.04}](Nb_{0.85}Ta_{0.15})O_3$–$xBiFeO_3$ ceramics, Journal of Alloys and Compounds 518 (2012) 1–5.
[7] J.G. Wu, D.Q. Xiao, Y.Y. Wang, Improved temperature stability of $CaTiO_3$-modified $[(K_{0.5}Na_{0.5})_{0.96}Li_{0.04}](Nb_{0.91}Sb_{0.05}\ Ta_{0.04})O_3$ lead-free piezoelectric ceramics, Journal of Applied Physics 104 (2008) 024102.
[8] H.L. Du, W.C. Zhou, F. Luo, Phase structure, dielectric properties, and relaxor behavior of $(K_{0.5}Na_{0.5})NbO_3$–$(Ba_{0.5}Sr_{0.5})TiO_3$ lead-free solid solution for high temperature applications, Journal of Applied Physics 105 (2009) 124104.
[9] H.L. Du, W.C. Zhou, F. Luo, New lead-free relaxor ferroelectrics derived from $(K_{0.5}Na_{0.5})NbO_3$ for high temperature applications, Ferroelectrics 401 (2010) 141–147.
[10] J.B. Zhao, H.L. Du, S.B. Qu, The effects of $Bi(Mg_{2/3}Nb_{1/3})O_3$ on piezoelectric and ferroelectric properties of $K_{0.5}Na_{0.5}NbO_3$ lead-free piezoelectric ceramics, Journal of Alloys and Compounds 509 (2011) 3537–3540.
[11] H.L. Cheng, H.L. Du, W.C. Zhou, $Bi(Zn_{2/3}Nb_{1/3})O_3$–$(K_{0.5}Na_{0.5})NbO_3$ high-temperature lead-free ferroelectric ceramics with low capacitance variation in a broad temperature usage range, Journal of the American Ceramic Society 96 (2013) 833–837.
[12] R.Z. Zuo, M. Wang, B. Ma, Sintering and electrical properties of $Na_{0.5}K_{0.5}NbO_3$ ceramics modified with lanthanum and iron oxides, Journal of Physics and Chemistry of Solids 70 (2009) 750–754.
[13] H.L. Cheng, H.L. Du, W.C. Zhou, Effects of $LaFeO_3$ additions on the dielectric and ferroelectric properties of $(K_{0.5}Na_{0.5})NbO_3$ ceramics, Journal of Inorganic Materials 27 (2012) 1228–1232.
[14] Z.H. Yao, H.X. Liu, M.H. Cao, Effects of Mn doping on the structure and electrical properties of high-temperature $BiScO_3$–$PbTiO_3$–$Pb(Zn_{1/3}Nb_{2/3})O_3$ piezoelectric ceramics, Materials Research Bulletin 46 (2011) 1257–1261.
[15] S. Zhang, E. Alberta, R. Eitel, C. Randall, T. Shrout, Elastic, dielectric and piezoelectric characterization of modified $BiScO_3$–$PbTiO_3$ ceramics, IEEE Transactions on Ultrasonics Ferroelectrics and Frequency Control 52 (2005) 2131–2139.
[16] C.W. Ahn, H.C. Song, S. Nahm, S.H. Park, K Uchino, Effect of MnO_2 on the piezoelectric properties of $(1-x)(Na_{0.5}K_{0.5})NbO_3$–$xBaTiO_3$ ceramics, Japanese Journal of Applied Physics 44 (2005) L1361–L1364.
[17] D.M. Lin, Q.J. Zheng, K.W. Kwok, Dielectric and piezoelectric properties of MnO_2-doped $K_{0.5}Na_{0.5}Nb_{0.92}Sb_{0.08}O_3$ lead-free ceramics, Journal of Materials Science: Materials in Electronics 21 (2010) 649–655.
[18] D. Lin, K.W. Kwok, H.L. Chan, Effects of MnO_2 on the microstructure and electrical properties of $0.94(K_{0.5}Na_{0.5})NbO_3$–$0.06Ba(Zr_{0.05}Ti_{0.95})O_3$ lead free ceramics, Materials Chemistry and Physics 109 (2008) 455–458.
[19] J.G. Hao, Z.J. Xu, R.Q. Chu, Y.J. Zhang, Effects of $K_4CuNb_8O_{23}$ on the structure and electrical properties of lead-free $0.94(Na_{0.5}K_{0.5})NbO_3$–$0.06LiNbO_3$ ceramics, Materials Research Bulletin 44 (2009) 1963–1967.
[20] D.M. Lin, K.W. Kwok, H.L.W. Chan, Microstructure, dielectric and piezoelectric properties of $(K_{0.5}Na_{0.5})\ NbO_3$–$Ba(Ti_{0.95}Zr_{0.05})O_3$ lead-free ceramics with CuO sintering aid, Applied Physics A 88 (2007) 359–363.

[21] L. He, C. Li, Effects of addition of MnO on piezoelectric properties of lead zirconate titanate, Journal of Materials Science: Materials in Electronics 35 (2000) 2477–2480.

[22] E. Li, H. Kakemoto, S. Wada, T. Tsurumi, Effects of manganese addition on piezoelectric properties of the (K,Na,Li)(Nb,Ta,Sb)O_3 lead-free ceramics, Journal of the Ceramic Society of Japan 115 (2007) 250.

[23] Q.Y. Yin, S.G. Yuan, Q Dong, Effect of CuO and MnO_2 doping on electrical properties of $0.92(K_{0.48}Na_{0.54})NbO_3$–$0.08LiNbO_3$ under low-temperature sintering, Journal of Alloys and Compounds 491 (2010) 340–343.